Supplement of Biogeosciences Discuss., 12, 6757–6781, 2015
http://www.biogeosciences-discuss.net/12/6757/2015/
doi:10.5194/bgd-12-6757-2015-supplement

Biogeosciences
Discussions
Open Access

Supplement of

Enhanced pH up-regulation enables the cold-water coral *Lophelia pertusa* to sustain growth in aragonite undersaturated conditions

M. Wall et al.

Correspondence to: M. Wall (mwall@geomar.de)

Material and Methods:

The corals were cultured under the conditions described in Form & Riebesell (Form and Riebesell, 2012) and summarized in Table S1. These conditions are used to calculate pK_B (pK_B= 8.795 for the natural in situ grown skeletal and pKB = 8.814 for the treatment corals) and translate skeletal $\delta^{11}B$ values of the different transects (#1-7) into internal calcifying fluid pH (pH_{cf}) in Table S2.

Table S1: Summarized cultural conditions from Form & Riebesell(Form and Riebesell, 2012) applicable to the specimens and skeletal regions analyzed.

	Sula reef	**Cultured CRSI**	**Cultured CRSII**	**Cultured CRSIII**
Temperature (^{o}C)	7,5	7.5±0.1	7.5±0.1	7.5±0.1
Salinity (PSU)	35,2	34.5±0.5	34.5±0.5	34.5±0.5
Depth (m)	285	n/a	n/a	n/a
Total alkalinity (µmol/kg)	2313,7	2298.5 ± 73.0	2232.4 ± 61.4	2349.9 ± 79.5
DIC (µmol/kg)	2149,8	2185.8 ± 82.6	2161.1 ± 71.2	2300.1 ± 89.2
$pH_{free\ scale}$	8,081	7.944 ± 0.064	7.829 ± 0.053	7.755 ± 0.056
***p*CO2 (µatm)**	405	604 ± 105	778 ± 112	982 ± 146
HCO_3^-	2009,3	2067.4 ± 83.8	2056.3 ± 70.8	2192.3 ± 87.0
Ω_{Ar}	1,74	1.366 ± 0.156	1.035 ± 0.090	0.932 ± 0.097

Results:

Table S2: Average $\delta^{11}B$ values for the different transects (# from respective figure in the manuscript and supplements) and skeletal regions, which were converted into internal calcifying fluid pH (pH_{cf}). All values are mean and standard deviation in brackets.

Transect	#1	#2	#3	#4	#5	#6	#7	∅ natural	∅ CRSIII
$\delta^{11}B$ primary skeleton	22.33 (1.40)	22.55 (1.78)	22.87 (2.02)	24.81 (1.39)	24.14 (0.98)	21.37	23.70 (2.02)	**22.48 (1.58)**	**24.52 (1.21)**
$\delta^{11}B$ secondary skeleton	26.90 (1.84)	29.17 (2.69)	28.09 (2.30)		27.10	28.06 (1.83)		**26.97 (4.73)**	**27.80 (1.94)**
pH_{cf} primary skeleton	8.58 (0.09)	8.59 (0.12)	8.61 (0.14)	8.76 (0.09)	8.71 (0.06)	8.51	8.69 (0.14)	**8.58 (0.11)**	**8.74 (0.08)**
pH_{cf} secondary skeleton	8.88 (0.12)	9.03 (0.18)	8.95 (0.15)		8.91	8.95 (0.12)		**8.94 (0.15)**	**8.95 (0.13)**

Visualizing the growth of the skeleton during natural and treatment conditions by tracing the Alizarin staining line.

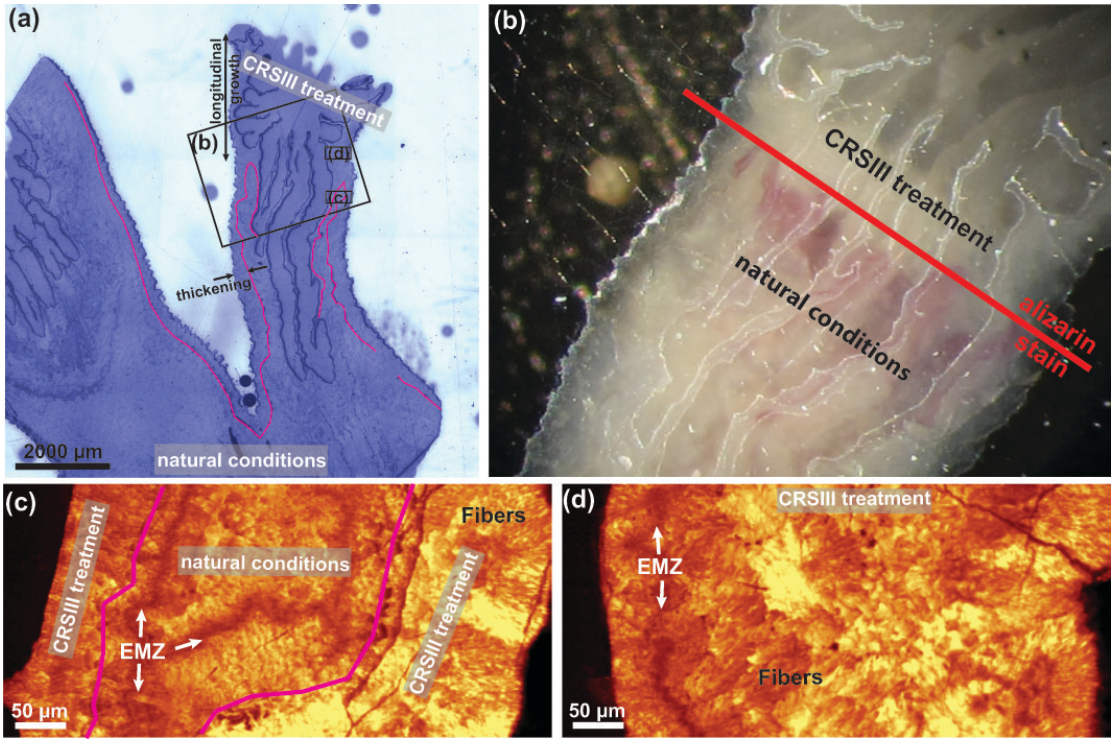

Figure S1: (a) *Lophelia pertusa* cut in longitudinal plane through an old and younger colony branch. Pink line outlines the position of the staining lines and separates the skeleton grown under natural and high CO_2 treatment conditions (CRSIII pCO_2 = 982). (b) Close-up of side branch and location of the staining edge above all skeleton was formed during treatment conditions. c,d) Raman map of the intensity distribution of the main aragonite peak (symmetric stretch, 1085 cm^{-1}) reveals the early mineralization zone (EMZ), the primary skeleton and the area of secondary thickening precipitated for both natural and treatment conditions.

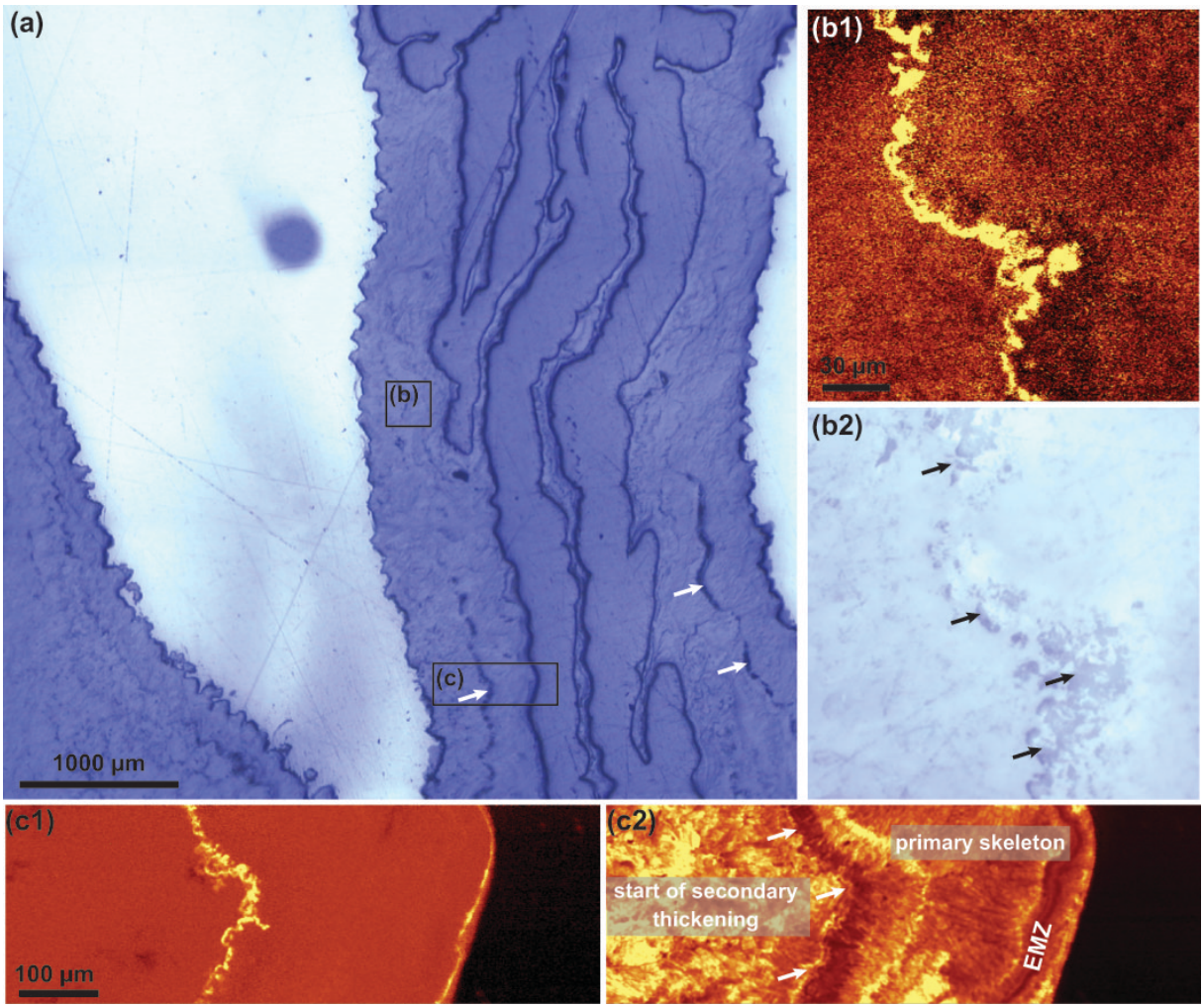

Figure S2: (a) *Lophelia pertusa* cut in longitudinal plane displays the location of Raman maps and microscopic image (50x). (b) Raman map of the staining line (b1) and the growth interruptions (black arrows) shown in the microscopic image (b2). (c) Raman maps of the location of the staining line (c1) and the growth interruption seen in aragonite orientation map (c2).

Even though the staining line is not visible in the microscopic image, traces of Alizarin were incorporated in the skeleton and lead to a disruption in fibre orientation and skeletal formation (see electronic supplementary material Fig. S2, which is visible by microscopic image Fig. S2a,b2).

Additional $\delta^{11}B$ transects display the variation of $\delta^{11}B$ with the coral growth growth stage, i.e. primary to secondary skeleton formation towards the outer rim and the influence of Alizarin staining.

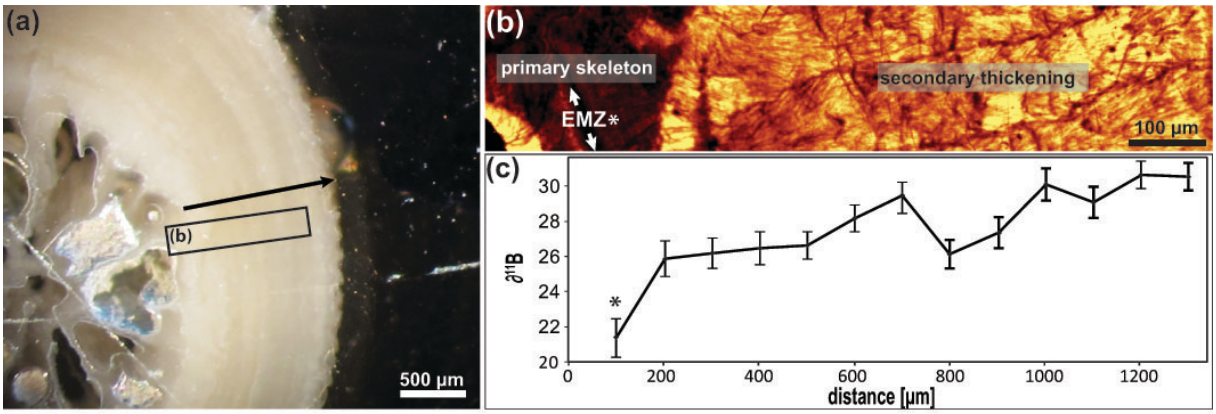

Figure S3: Old branch of *Lophelia pertusa* cut in transversal plane and prepared for Raman mapping and SIMS analysis. (a) Microscopic image contains the location of the Raman map and the SIMS transects. (b) Raman map of the intensity distribution of the main aragonite peak (symmetric stretch, 1085 cm^{-1}) reveals the early mineralization zone (EMZ), the primary skeleton and the area of secondary thickening. Asterisks mark EMZ in the primary skeleton. c) $\delta^{11}B$ measured from inside to the outer coral skeletal rim (transect #6)

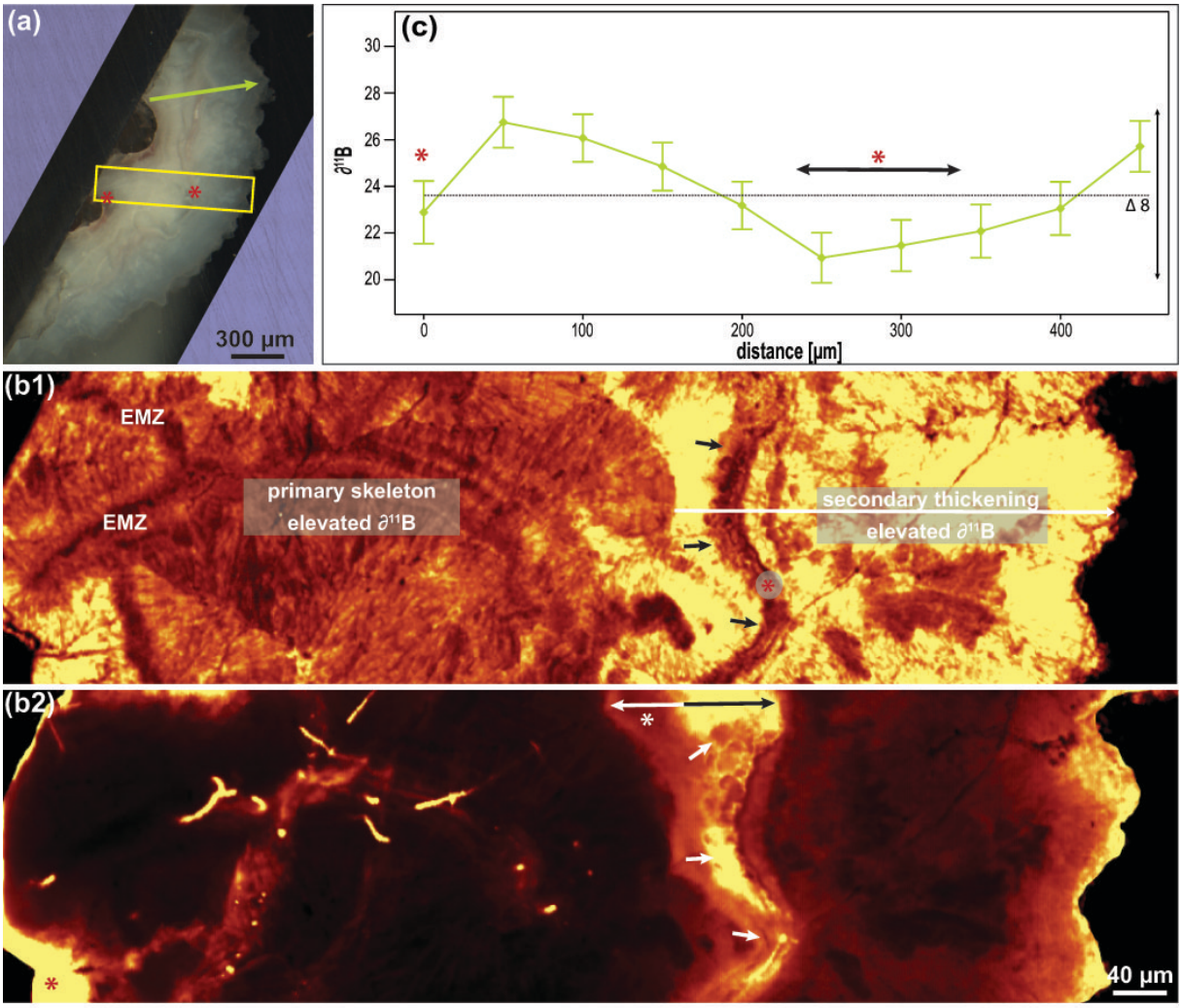

Figure S4: Young branch of *Lophelia pertusa* cut in transversal plane and prepared for Raman mapping and SIMS analysis. (a) Microscopic image contains the location of the Raman map and the SIMS transects. Red asterisks mark the location of the staining line. (b) Raman map of the intensity distribution of the main aragonite peak (symmetric stretch, 1085 cm^{-1}) reveals the early mineralization zone (EMZ), the primary skeleton and the area of secondary thickening. Arrows mark the skeletal growth interruption at the staining

line. (b2) Raman fluorescence map displays the location of the staining line and difference in width. c) $\delta^{11}B$ measured from inside to the outer coral skeletal rim (transect #7)

Discussion:

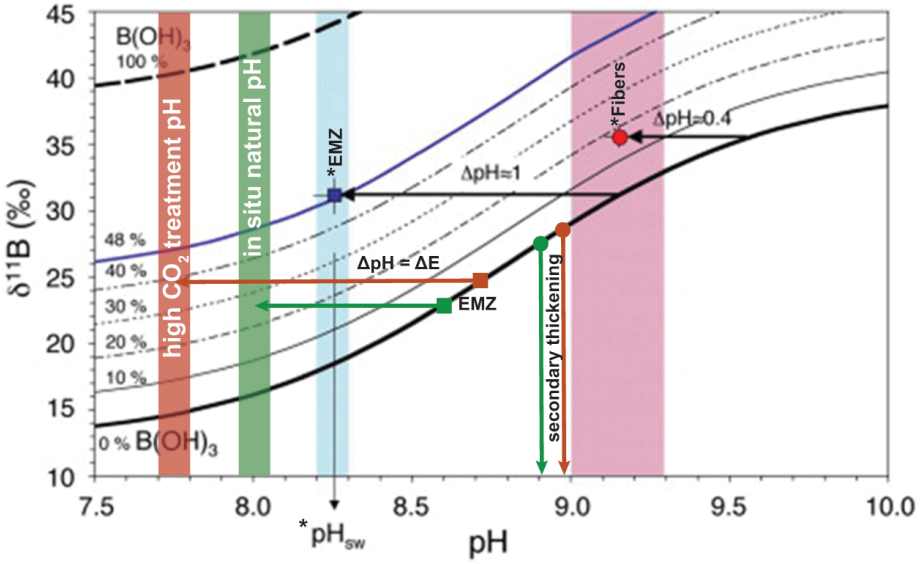

Figure S5: $\delta^{11}B$ data for the primary and secondary skeleton plotted into the $\delta^{11}B$-pH dependency plot (modified **from** (Rollion-Bard et al., 2011)). Differences in the proportions of incorporated borate ($B(OH)_4^-$) and boric acid ($B(OH)_3$) could potentially account for observed variations in $\delta^{11}B$ and deviation from reconstructed seawater pH. A previous study (Rollion-Bard et al., 2011) found that 18% boric acid was incorporated into the fibers (*Fibers) and 48% into the EMZ (*EMZ). Accounting for the boric acid incorporation allowed the reconstruction of seawater pH (*pHsw) from the EMZ. Our data do not allow the seawater pH reconstruction using 48% boric acid content and indicate differnt boric acid content for the natural in situ growth and the high CO_2 treatment.

References

Form, A. U. and Riebesell, U.: Acclimation to ocean acidification during long-term CO2 exposure in the cold-water coral Lophelia pertusa, Glob. Chang. Biol., 18(3), 843–853, doi:10.1111/j.1365-2486.2011.02583.x, 2012.

Rollion-Bard, C., Blamart, D., Trebosc, J., Tricot, G., Mussi, A. and Cuif, J.-P.: Boron isotopes as pH proxy : A new look at boron speciation in deep-sea corals using 11 B MAS NMR and EELS, Geochemica Cosmochem. Acta, 75, 1003–1012, doi:10.1016/j.gca.2010.11.023, 2011.